Journal of Zhejiang University SCIENCE A
ISSN 1673-565X (Print); ISSN 1862-1775 (Online)
www.zju.edu.cn/jzus; www.springerlink.com
E-mail: jzus@zju.edu.cn

Flat-type permanent magnet linear alternator: A suitable device for a free piston linear alternator*

Qing-feng LI†, Jin XIAO, Zhen HUANG

(*MOE Key Laboratory for Power Machinery and Engineering, Shanghai Jiao Tong University, Shanghai 200240, China*)

†E-mail: qfli@sjtu.edu.cn

Received Mar. 26, 2008; Revision accepted Aug. 11, 2008; Crosschecked Nov. 13, 2008

Abstract: We proposed the flat-type permanent magnet linear alternator (LA) for free piston linear alternators (FPLAs) instead of the tubular one. Using the finite element method (FEM), we compare these two kinds of LAs. The FEM result shows that the flat-type permanent magnet LA has higher efficiency and larger output specific power than the tubular one, therefore more suitable for FPLAs, and that the alternator design can be optimized with respect to the permanent magnet length as well as the air gap.

Key words: Free piston (FP), Linear alternator (LA), Internal combustion engine (ICE), Finite element method (FEM)
doi:10.1631/jzus.A0820224 **Document code:** A **CLC number:** TN929.5

INTRODUCTION

Nowadays, as people are more concerned with the side effects caused by automobiles, such as fossil fuel shortages and global environment problems, their research is slowly transferred to new fuels, and environmentally friendly and highly efficient automotive drive systems. Hybrid electric vehicle (HEV) —with high efficiency and low emission—seems to be the best solution for this crisis. But the present state of battery technology severely limits the range of pure electric vehicles. Until significant advances in battery technology are made can hybrid propulsion systems only provide an interim solution (Cawthorne *et al*., 2001). Under this situation appears the free piston linear alternator (FPLA), which is regarded as one of the right devices to meet the standard (Goldsborough and van Blarigan, 1999; van Blarigan, 2002). The FPLA is the combination of free piston internal combustion engine (FPICE) and the linear alternator (LA), integrating the advantages of the two parts. This machine has only one moving part and suffers less from the friction force due to no side loads. The piston motion is not constrained so that the compression ratio is variable, making the high compression ratio and multi-fuel type easily achieved. Moreover, it also makes the modern combustion technique (homogeneous charge compression ignition, HCCI) possible. As another main part of FPLA, the LA is capable of directly utilizing the linear piston force without any need of the additional mechanical components that are necessary in a rotary configuration. FPLA is thus an effectively integrated energy conversion device.

Many works on FPLA have been carried out since 1998. Clark at West Virginia University (WVU) established an FPLA prototype with a bore of 36.5 mm and the maximum possible stroke of 50 mm, using gasoline as the fuel. The engine had a peak output electric power of 316 W with the frequency of 23.1 Hz (Atkinson *et al.*, 1999). This is the most successful running prototype data that can be found. van Blarigan (2002) at Sandia National Laboratories (SNL) did a series of single shot combustion experiments on the Rapid Compression Expansion Machine to simulate the FP motion. According to their experiments, the FPICE under the ratios of high

* Project (No. 50806046) supported by the National Natural Science Foundation of China

compression (about 30:1) and low equivalence ($\Phi\approx0.35$) could reach the thermal efficiency of 56% and very low NO_x and HC emissions (Goldsborough and van Blarigan, 1999; van Blarigan, 2002). A research group from Royal Institute of Technology (KTH) did lots of works on transversal flux machine used in an FPLA. Based on their work, FPLA benefited from a low translator mass compared to other permanent magnet configurations but suffered from a low power factor and high manufacturing costs (Arshad *et al.*, 2002; 2003), so it was still under further investigation. For more comprehensive descriptions of above applications, refer to (Li *et al.*, 2008).

The previous studies show that the flat-type LA is rarely used in FPLA and indeed inferior to the tubular-type one in terms of structural merits. The rotation of the piston does not affect the electric characteristics of the linear generator and the amount of the leakage flux is small (Cosic *et al.*, 2003). But the magnetic ring, lamination stacked stator and the windings in tubular stator are hard to be manufactured and assembled. Besides that, sectional areas of the windings are constrained by the magnetic ring. The flat-type one is, however, free of these weaknesses and yields much bigger output power than that of the tubular one; therefore it can be used in FPLA simply by some mechanical instrument to constrain the piston's rotation motion. This paper presents a comparative study on these two types of LA. After the finite element models are established, the peak voltage, current density, specific power, as well as the efficiency of the two alternators are compared. Results show that although constrained by the structure drawback, the flat-type alternator has higher efficiency, specific power, output voltage and current. The flat-type LA is thus much suitable for FPLA.

DESCRIPTION OF THE FPLA

As the cross-sectional view shown in Fig.1, the FPLA consists of two parts. One is FPICE, which contains dual opposed pistons, connected by a connecting rod and two relevant cylinders. The other is the LA with the permanent magnet (PM) mounted on the connecting rod as the translator. The back iron and the windings are arranged in the stator. Combustion occurs alternately in each cylinder, making the connecting rod move back and forth. Then the flux linked with circular wound coils changes periodically to produce the electromotive force (EMF).

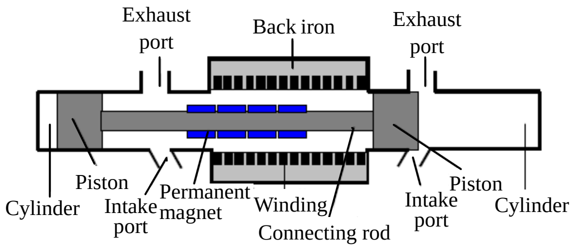

Fig.1 Cross-sectional view of FPLA

This small-scale generator can be used in power generation or HEV, providing a new concept in ICE revolution.

LINEAR ALTERNATOR DESIGN AND MODELING

As mentioned above, finding a suitable LA to match the FPICE is crucial to the design process. Basically, there are two kinds of LA, the flat-type and the tubular-type. Both of them can be treated as an alternator cutting and unrolling from a rotary one (Boldea and Nasar, 1999). The only difference is that the rotary alternator uses sinusoidal magnetic field to produce sinusoidal voltage while the linear one exploits sinusoidal velocity. According to their excitation method, LAs are divided into three kinds, i.e., induction, PM and reluctance ones. As strong magnetic field can be generated by rare-earth PMs, and the mechanical structure of PM LA is simple, LAs are used widely in FPLA.

Modeling

The basic geometric design approach for an LA is provided in (Boldea and Nasar, 1987). Since the piston stroke is small and may be used in HEV, only the 1-phase machine is studied in this paper. Boldea and Nasar (1987) suggested that the pole pitch should have the same length as the stroke while the tooth width and the slot width should be half of it. Under this geometry, the EMF will have the same frequency as the primary engine. The inner diameter of the LA and the number of turns are decided by the output power and voltage. The first parameter can be determined using

$$D = \frac{1}{\pi m_r \tau f_{xy}} \cdot \frac{S_n}{u\eta}, \tag{1}$$

where S_n is rated power of the alternator, m_r the number of poles, τ the pole pitch, f_{xy} the specific thrust which in general ranges from 1.0 to 1.5 N/cm^2, u the rated translator velocity, and η the rated efficiency.

The number of turns per slot can be determined from

$$n_s = \frac{\sqrt{2}V_{out}}{2\omega_1 B_{gr} \tau D}, \tag{2}$$

where V_{out} is EMF, ω_1 the angular frequency, and B_{gr} the magnet air gap flux density which ranges from 0.6 to 0.7 T for a rare-earth PM.

From abovementioned, the parameters and geometric dimensions of the tubular machine are obtained as shown in Table 1. According to the actual application condition, the N38SH is used as the PM material, and WDG-50-1 is used as the stator core and the translator material.

Table 1 Tubular alternator parameters

Parameter	Value
Output power S_n (W)	500
EMF V_{out} (V)	100
Number of poles m_r	4
Pole pitch τ (mm)	37.4
Diameter D (mm)	30
Tooth width b_t (mm)	18.7
Slot width b_s (mm)	18.7
Air gap h_g (mm)	1
Number of turns n_s	100
Slot depth h_s (mm)	16
PM length L (mm)	30
PM gap W (mm)	7.4
Frequency f (Hz)	50

The model of the tubular alternator is shown in Fig.2 and this structure is widely used in the referred FPLA prototypes. Four radially magnetized PMs are mounted on the translator and importantly, the adjacent PMs are magnetized in the opposite direction. The translator reciprocates relative to radially inboard stator coils, thereby the flux imposes on the windings to induce a voltage.

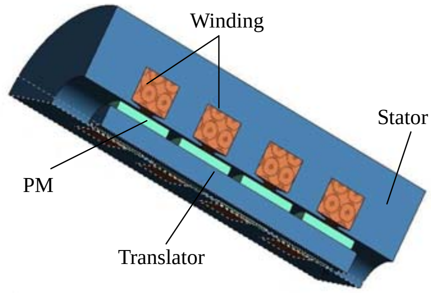

Fig.2 Model of tubular linear alternator

For comparison, the cross-section of the flat-type alternator is set the same as that of the tubular alternator, as illustrated in Fig.3. Besides that, this section extrudes to 100 mm to match the length in the tubular one. Under these geometries, the translator mass of the flat alternator is nearly 4 times larger than that of the tubular one.

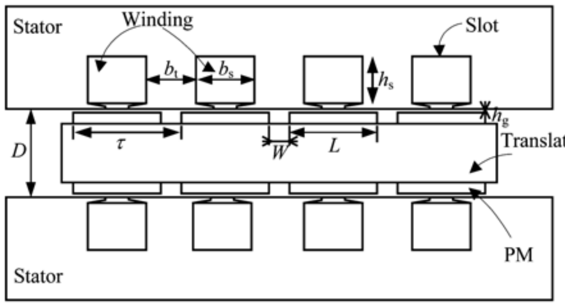

Fig.3 Cross-section of flat-type linear alternator whose parameters are the same as in Table 1

Double stators are accepted to eliminate the magnetic attraction between PMs and the stator teeth. Two windings are arranged up the translator perpendicular while the other two under the translator, and these four windings are altogether connected in series. Note that only half of the prototype is simulated to save the computation time.

Finite element analysis and comparison

After the two models are successfully established, the finite element method (FEM) is used to analyse the built models to get the thrust force, the output voltage, the stator current, the ohmic loss and the iron loss, etc.

Fig.4 illustrates the output parameters comparison between the two types of alternator under the same load. The translator masses of flat-type and tubular alternators are 1.49 and 0.625 kg, respectively. The specific power for flat-type alternators is 0.53 kW/kg while that for tubular ones is 0.37 kW/kg. Although the flat-type alternator has a larger moving mass, its specific power is about 43% larger than that of the tubular one. This may mainly because the flat-type benefits in the magnetic excitation, and furthermore, the efficiency of the flat-type alternator is about 2% higher than that of the tubular one. It is clear that the flat-type alternator output voltage is higher than the tubular one. As the magnetic ring used in the tubular alternator is expensive for custom-designed dimensions (Cawthorne *et al.*, 2001), the winding areas for tubular alternator are constrained by the purchased PM rings. But the magnetic stick used in the flat-type alternator does not have this problem so the stator section areas are bigger. This ensures a bigger flux linkage.

According to the Faraday law, the EMF can be written as

$$\varepsilon = n\cdot\frac{\mathrm{d}\varphi}{\mathrm{d}t} = n\cdot\frac{\mathrm{d}\varphi}{\mathrm{d}x}\cdot\frac{\mathrm{d}x}{\mathrm{d}t}, \tag{3}$$

where n is the number of turns, φ the flux of each coil, and x the translator displacement. During this analysis, the number of turns and the velocity profile in the two models are the same, so the EMF is only determined by $\frac{\mathrm{d}\varphi}{\mathrm{d}t}$.

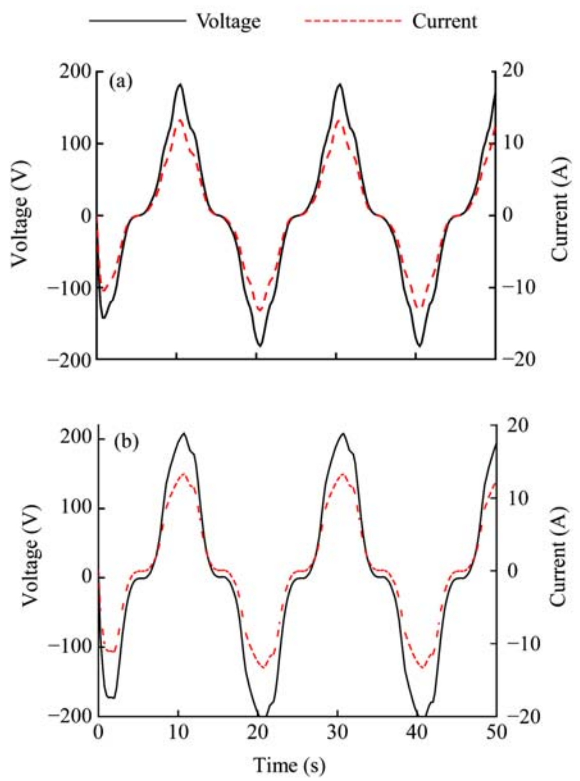

Fig.4 Flat-type (a) and tubular-type (b) output performance

Fig.5 plots the flux vs the displacement for half stroke, and the flux curve is linear in the central part. Using linear fit, the slope of flat-type alternator is nearly two times that of the tubular alternator, and therefore the EMF of the two models has the same proportion. To these two models, the stator resistance is very small, so the larger EMF is beneficial to higher output voltage and power.

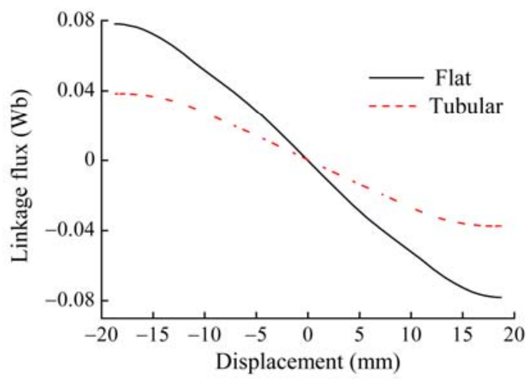

Fig.5 Linkage flux vs the stroke

Towards the left and right ends of strokes, the flux curve is no longer linear but changes slightly because of the flux leakage. At these two positions, the translator speed reversal follows the output voltage. The output voltage then stays zero for a while which as shown in Fig.4. It is so called the dead zone that may result in the delivered power pulsates and torque ripple in the propelling HEV (Hansson *et al.*, 2005). To smoothen these pulsations, an additional energy storage device could be used. Since the cause of the dead zone is clear, it can be avoided fundamentally. Generally speaking, the effective way to avoid it is constraining the translator stroke into the central part of piston stroke in Fig.5. Usually, there are two methods. The first one is widening the PM length (Yang *et al.*, 2006) and the second one is reducing the translator's working scale. Since the translator is propelled by FPICE while the main characteristic of this engine is that the piston stroke is not constrained, the second method can be achieved easily. Based on the dynamic simulation process of the FPICE, one can reduce the piston stroke by advancing the ignition position, alleviating the intake pressure or lessening fuel mass.

Fig.6 is the output comparison of two different stroke lengths. Curve 1 represents the output voltage under possible maximum stroke of 37.4 mm while Curve 2 illustrates the stroke of 32 mm. As can be seen, the dead zone in Curve 2 disappears as the stroke decreases. During this simulation, a constant frequency velocity profile with a sinusoidal-shape is assumed. Reducing the piston stroke actually means decreasing the peak velocity, which leads to the slight decline of output voltage according to Eq.(3).

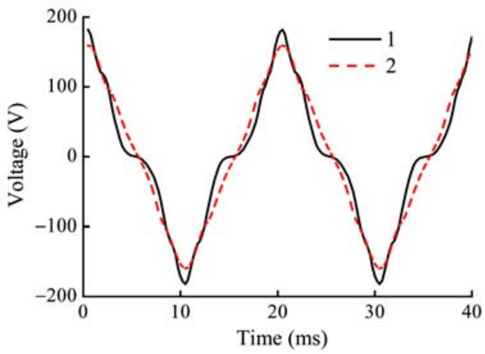

Fig.6 Output as a function of time and stroke

Performance analysis

Given that people are more concerned with the efficiency and the specific power for the energy device of HEV, a comparison between the two established models is performed in this part. In the following analysis, the velocity profile is set to match the possible maximum stroke. The flux excitation and the EMF as well keep constant in this way.

From the equivalent circuit of the alternator, the instantaneous output power can be calculated as

$$\dot{P}_{\text{out}} = u \cdot i = \left| \frac{\varepsilon}{r + R_1 + jX} \right|^2 \cdot R_1 = \frac{\varepsilon^2}{(r + R_1)^2 + X^2} \cdot R_1, \tag{4}$$

where r and X are the stator resistance and inductance, respectively, and R_1 is the external resistance load. The output power is only related to the external load and the stator resistance. Compared with the external resistance, the stator resistance is small enough to neglect, then the output power nearly takes an inverse proportion to the external resistance.

The efficiency of linear alternator can be written as

$$\eta = \frac{\overline{P}_{\text{out}}}{\overline{P}_{\text{in}}} = \frac{\overline{P}_{\text{out}}}{\overline{P}_{\text{out}} + \overline{P}_{\text{ohmic}} + \overline{P}_{\text{iron}}} \times 100\%, \tag{5}$$

where P_{in}, P_{iron} and P_{ohmic} are input power, stator iron loss and stator copper loss, respectively. As the output resistance increases, the stator current decreases while the stator and magnetic ohmic loss reduces. The thrust force, proportional to the active component of current, decreases as well. So both the P_{in} and P_{ohmic} decrease. The P_{iron} that is calculated at a certain excitation frequency (usually 60 Hz) can be obtained by Infolytica Magnet software. Then the needed iron loss can be obtained through a correction equation.

The output voltage, current, ohmic loss and iron loss under different external loads can be obtained from FE model. Then the specific power and efficiency can be calculated from Eq.(4) and Eq.(5), respectively. The plots of specific power and the efficiency vs external loads are shown in Fig.7. It is obvious that the two types of alternators have the same trends when external load changes just as analyzed before. But the specific power of the flat-type alternator is a bit higher than that of the tubular one. Since the efficiency is controlled by three parameters, as the external resistance increases, it rises first and then falls down rapidly. The rising is due to the fact that at first the external resistance is very small and the stator current is big. So the stator ohmic loss is huge, but it reduces rapidly as the external resistance increases slightly. The efficiency falls down as the external load increases further, because at this level, the external resistance is big enough and the output power decreases rapidly while the two losses nearly keep constant. It is obvious that the efficiency of flat-type alternator is larger than that of the tubular one. The peak values of flat-type and tubular alternators are 95.8% and 93.9%, respectively.

Based on the above analysis, although showing lower structural performance, the flat-type LA has higher efficiency, output power and current density as well as simple manufacturing technology. All these advantages make it used in FPLA reasonable. For this established model, the specific power changes as the external loads change, and it can reach 0.91 kW/kg while the efficiency is above 95%. The output voltage can reach 180 V while the current density is above 2 A/mm^2.

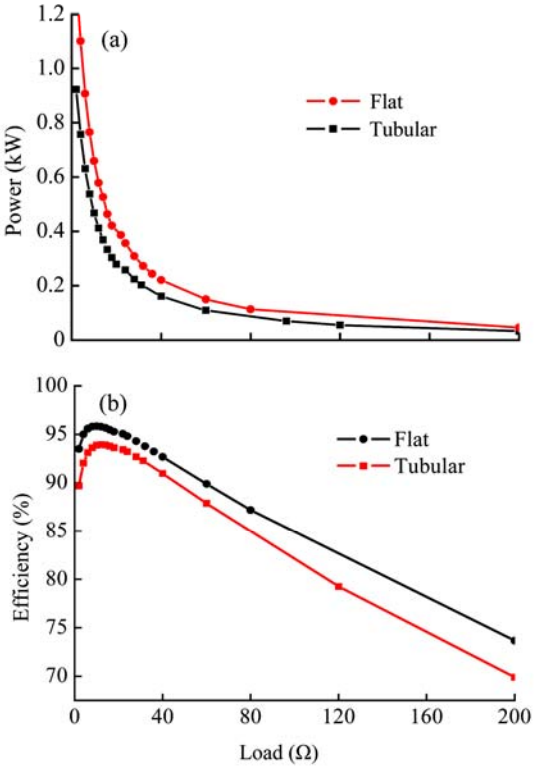

Fig.7 Specific power (a) and efficiency (b) vs external load

A supporting carriage is provided under the translator to make up its structure defect. It can eliminate the rotational motion as well as support the translator's gravity. This also makes sure that the side loads on piston ring are small. A schematic graph of the carriage is shown in Fig.8. The translator travels above the two wheels, and its motion is restricted by the rail. The carriage and the stator are fixed to the base through vibration buffer-layer.

Table 2 summarizes the major performance of MH-Ni battery for HEV made by GM Co. (USA) and VARTA Co. (Germany) (Ma and Xia, 2003). It is clear that the flat-type of alternator can easily reach its standards.

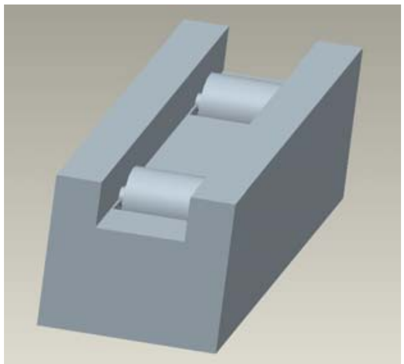

Fig.8 Schematic graph of the carriage

Table 2 Major performance of MH-Ni battery for HEV

Performance	GM Co.		VARTA Co.	
	C=20	*C*=60	*C*=10	*C*=4
Number of cells	6	13	1	1
Cell voltage (V)	7.2	13.2	1.2	1.2
Mass (kg)	4.3	12.2	0.19	0.09
Specific power (kW/kg)	0.55	0.6	0.85	0.3

C is capacity (A·h)

Furthermore, the alternator, stable and free of charging and discharging influence, is hence the right device for the HEV. But compared with Li-ion battery nowadays used in HEV, the flat-type LA shows low performance as the Li-ion battery can reach a specific power higher than 1 kW/kg. The LA still needs to be further investigated to meet the HEV requests.

Optimal design

The translator as a part of the connecting rod is directly driven by the FPICE, therefore can be modified to improve the engine performance. Adjusting the PM length is seemingly an effective way to obtain the optimal output power as well as modifying the moving mass. Another important factor to improve the alternator performance is optimizing the air gap. Fig.9 presents the alternator performance as a function of PM length and air gap.

During this study, the sum of *W* and *L* is set equal to the pole pitch. When the PM length grows from 28 to 34 mm (*W*/*L* changes from 0.336 to 0.1), the output power increases while the tendency becomes mitigated. The peak efficiency occurs when PM length is around 30 mm. The longer PM length has no infinite improvement for the performance. When L is widened over a certain range, the magnetic reluctance between the adjacent PMs will reduce and the flux short will increase. The efficiency then drops and the performance of the LA becomes poor. Considering the costs, the output power, and the alternator efficiency, the 32 mm PM length is chosen. The total mass of the translator goes to 3 kg.

As the air gap decreases from 2.5 to 1.0 mm, the output power increases significantly. Although a smaller air-gap length would improve the output power, its limitations come from manufacturing tolerances, the stiffness, and the static and dynamic radial run-out of the moving-magnet armature (Wang *et al.*, 2007). Based on our processing technology, the selected optimal value for the air gap is 1.0 mm.

Under these two optimal parameters, the plot of output power vs external load (Fig.10) only establishes the loads under which the alternator efficiency is above 95%.

Fig.11 shows the peak thrust force as a function of the peak machine current. The thrust constant, useful in modifying the engine dynamic simulation, is about 36.3 N/A.

Fig.12 presents the external characteristic of the alternator (voltage vs current). Due to the stator inductance, its external characteristic is not linear. It is a kind of synchronous alternators.

CONCLUSION

FPLA is a robust energy conversion device, integrating the advantages of FPICE and the LA. Investigation shows that this engine has a nature to build up compression ratio and improve the thermal efficiency (Shoukry *et al.*, 2002). With its applications in both stationary power generation and HEV, this device is an effective way to solve the energy crisis and the environment problem.

(1) The flat-type LA is much better than the tubular one in manufacturing process, specific power, efficiency, etc. It shows a better performance than the MH-Ni battery used in HEV.

(2) The flat-type LA is a kind of synchronous

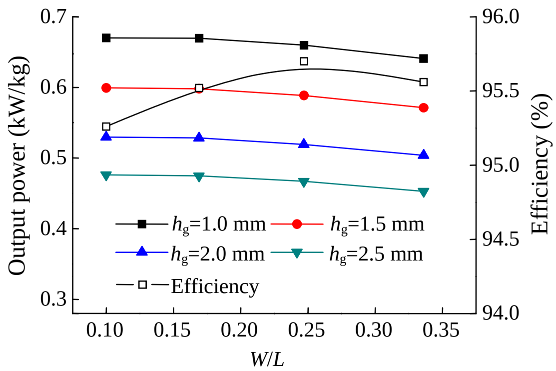

Fig.9 Performance as a function with *W*/L and air gap

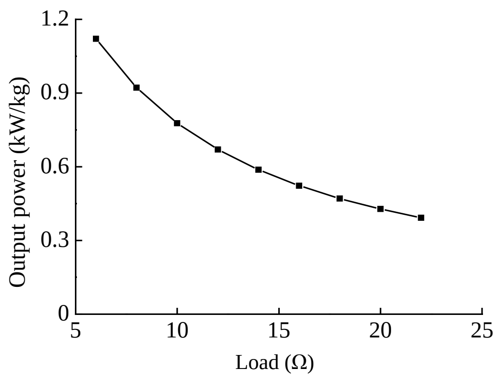

Fig.10 Specific power vs external load

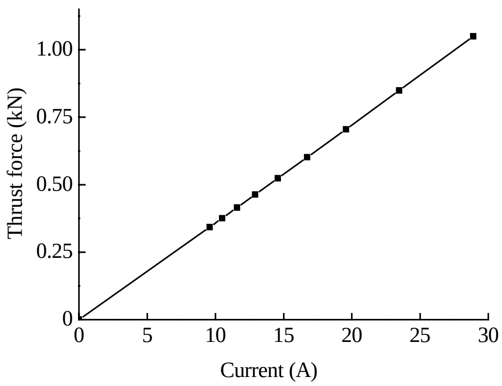

Fig.11 Thrust force vs current

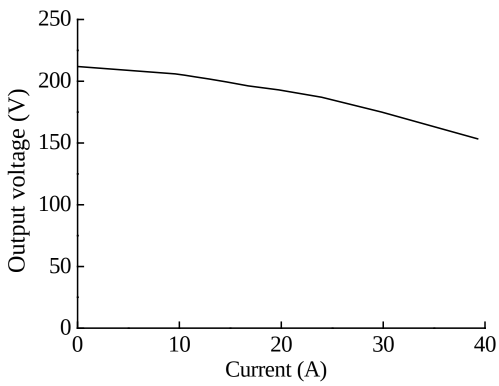

Fig.12 External characteristic of the alternator

alternators and the output pulsation can be eliminated effectively due to the special structure of FPICE.

(3) The design of the flat-type LA can be optimized with respect to the PM length and the air gap.

ACKNOWLEDGEMENTS

The authors would like to thank the assistance of Dr. Jian-hui Wang of Shanghai Jiao Tong University for the help in the development and implementation of the FE model of the linear engine. Dr. Wang has provided a great deal of guidance on the magnetic FE software.

References

Arshad, W.M., Sadarangani, C., Bäckström, T., Thelin, P., 2002. Finding an Appropriate Electrical Machine for a Free Piston Generator. The 19th Electrical Vehicle Symposium (EVS), Busan, Korea, p.427-437.

Arshad, W.M., Thelin, P., Bäckström, T., Sadarangani, C., 2003. Alternative Electrical Machine Solutions for a Free Piston Generator. Proceedings of the 6th International Power Engineering Conference (IPEC2003), Singapore, p.329-334.

Atkinson, C.M., Petreanu, S., Clark, N.N., Atkinson, R.J., McDaniel, T.I., Nandkumar, S., Famouri, P., 1999. Numerical Simulation of a Two Stroke Linear Engine-alternator Combination. SAE Technical Paper Series, No. 1999-01-0921, p.1-15.

Boldea, I., Nasar, S.A., 1987. Permanent-magnet linear alternators—Part II: design guidelines. *IEEE Transactions on Aerospace and Electronic Systems*, **23**(1):79-82. [doi:10.1109/TAES.1987.313338]

Boldea, I., Nasar, S.A., 1999. Linear electric actuators and generators. *IEEE Transactions on Energy Conversion*, **14**(3):712-717. [doi:10.1109/60.790940]

Cawthorne, W., Famouri, P., Clark, N., 2001. Integrated Design of Linear Alternator/Engine System for HEV Auxiliary Power Unit. IEEE International Conference on Electric Machines and Drives (IEMDC), p.267-274. [doi:10.1109/IEMDC.2001.939310]

Cosic, A., Lindback, J., Arshad, W.M., Leksell, M., Thelin, P., Nordlund, E., 2003. Application of a Free-Piston Generator in a Series Hybrid Vehicle. The 4th International Symposium on Linear Drives for Industry Applications, LDIA, p.541-544.

Goldsborough, S., van Blarigan, P., 1999. A Numerical Study of a Free Piston IC Engine Operating on Homogenous Charge Compression Ignition Combustion. SAE Technical Papers Series, No. 1999-01-0619, p.1-14.

Hansson, J., Leksell, M., Carlsson, F., 2005. Minimizing Power Pulsations in a Free Piston Energy Converter. IEEE 11th European Conference on Power Electronics and Applications, Dresden, Germany.

Li, Q.F., Xiao, J., Huang, Z., 2008. Simulation of a two-stroke free-piston engine for electrical power generation. *Energy & Fuels*, **22**(5):3443-3449. [doi:10.1021/ef800217k]

Ma, L.P., Xia, B.J., 2003. State of art of R&D of power Ni-MH battery for hybrid electric vehicle. *Chinese Journal of Power Sources*, **27**:245-249 (in Chinese).

Shoukry, E.F., Taylor, S., Clark, N., Famouri, P., 2002. Numerical Simulation for Parametric Study of a Two-stroke Direct Injection Linear Engine. SAE Technical Papers Series, No. 2002-01-1739.

van Blarigan, P., 2002. Advanced Internal Combustion Electrical Generator. Proceeding 2002 U.S. DOE Hydrogen Program Review, NREL/CP-610-32405, p.1-16.

Wang, J., West, M., Howe, D., La Parra, H.Z.-D., Arshad, W.M., 2007. Design and experimental verification of a linear permanent magnet generator for a free-piston energy converter. *IEEE Transactions on Energy Conversion*, **22**(2):299-305. [doi:10.1109/TEC.2006.875434]

Yang, B., Wen, J.B., Yang, G., Li, Q.X., 2006. Finite element analysis for the magnetic field and force of the linear permanent reciprocating generators. *Explosion-Proof Electric Machine*, **41**(3):28-31 (in Chinese).